

SCIENTIFIC REPORTS



OPEN

T cells display mitochondria hyperpolarization in human type 1 diabetes

Jing Chen¹, Anna V. Chernatynskaya¹, Jian-Wei Li^{1,3}, Matthew R. Kimbrell¹, Richard J. Cassidy^{1,4}, Daniel J. Perry¹, Andrew B. Muir², Mark A. Atkinson¹, Todd M. Brusko¹ & Clayton E. Mathews¹

T lymphocytes constitute a major effector cell population in autoimmune type 1 diabetes. Despite essential functions of mitochondria in regulating activation, proliferation, and apoptosis of T cells, little is known regarding T cell metabolism in the progression of human type 1 diabetes. In this study, we report, using two independent cohorts, that T cells from patients with type 1 diabetes exhibited mitochondrial inner-membrane hyperpolarization (MHP). Increased MHP was a general phenotype observed in T cell subsets irrespective of prior antigen exposure, and was not correlated with HbA1C levels, subject age, or duration of diabetes. Elevated T cell MHP was not detected in subjects with type 2 diabetes. T cell MHP was associated with increased activation-induced IFN γ production, and activation-induced IFN γ was linked to mitochondria-specific ROS production. T cells from subjects with type 1 diabetes also exhibited lower intracellular ATP levels. In conclusion, intrinsic mitochondrial dysfunction observed in type 1 diabetes alters mitochondrial ATP and IFN γ production; the latter is correlated with ROS generation. These changes impact T cell bioenergetics and function.

Increasing evidence suggests that type 1 diabetes patients exhibit immune dysregulation, most notably, a propensity towards pro-inflammatory innate immune activities and aberrant adaptive T cell responses¹. Despite this apparent deficit in immune tolerance, the cellular and molecular contributors to this process remain poorly characterized. The essential role of mitochondria in T cell activity has drawn great attention in recent years^{2,3}. Metabolic control of adaptive T cell activity likely plays a critical role in determining autoimmune disease progression or the maintenance of peripheral immune tolerance since, in these processes, mitochondrial metabolic activity plays a central role in controlling T cell activation, proliferation, and programmed cell death⁴.

In addition to providing energy for most human cells, mitochondria are also a major site for generation of reactive oxygen species (ROS). When T cells interact with antigen presenting cells (APCs) through HLA/antigen-T cell receptor (TCR) engagement, mitochondria within T cells are translocated to the region of the cytoplasm directly adjacent to the immunological synapse. At the immunological synapse, through a balanced process of fission and fusion, mitochondria maintain inner-membrane potential ($\Delta\Psi_m$), generate ATP, control local calcium concentrations, and produce mitochondrial ROS (mtROS)^{5,6}. This generation of mtROS is essential for IL-2 production and proliferation⁷. Therefore, mitochondria are not only the T cell powerhouse but also, essential for regulating cell signaling. Given these processes are known to play a role in controlling immune tolerance, it is possible that dysfunction of mitochondria could result in immune dysregulation and autoimmunity.

T cell mitochondrial dysfunction has been identified as a feature in multiple autoimmune diseases, including Systemic Lupus Erythematosus (SLE)⁸⁻¹⁰. In human SLE, the phenotype of persistent mitochondrial inner membrane hyperpolarization (MHP) is restricted to T cells. T cell MHP has been associated with elevated cellular ROS levels¹¹. Further, increased production of Nitric Oxide (NO) by monocytes is thought to be the mechanism for induction of T cell MHP in SLE patients¹². In type 1 diabetes, studies linking mitochondrial defects to disease are near exclusively limited to murine models where mitochondrial control of autoimmunity has been linked with dysregulated T cell apoptosis. Indeed, in both diabetes-prone NOD mice and BB-DP rats, genetic susceptibility

¹Department of Pathology, Immunology, and Laboratory Medicine, University of Florida, Gainesville, FL, USA.

²Department of Pediatrics, Emory University, Atlanta, GA, USA. ³Present address: Department of Endocrinology and Metabolism, West China Hospital of Sichuan University, Chengdu, 610041, China. ⁴Present address: Department of Radiation Oncology, Emory University, Atlanta, GA, USA. Correspondence and requests for materials should be addressed to J.C. (email: jic24@pathology.ufl.edu) or C.E.M. (email: clayton.mathews@pathology.ufl.edu)

regulates the expression of genes controlling mitochondrial apoptosis of T cells^{13,14}, resulting in autoimmunity. However, as noted, there is a paucity of studies of mitochondrial function or of metabolic control in T cells in human type 1 diabetes.

In this study, we first analyzed T cell $\Delta\Psi_m$ using peripheral blood mononuclear cells (PBMC) from type 1 diabetes patients and controls. We observed that T cells of all subsets from type 1 diabetes patients exhibit MHP, which is not associated with age, disease duration, or metabolic control of the subjects. We then confirmed this observation in enriched total T cells from a separate cohort, which included a group of patients with type 2 diabetes to determine whether T cell MHP is a consequence of abnormal glucose metabolism. Analyses indicated that T cells from patients with type 2 diabetes did not demonstrate T cell MHP. Functional studies provided evidence that T cell MHP was linked with altered mitochondrial and cytokine responses from T cells of patients with type 1 diabetes after TCR stimulation.

Results

Low dose DiOC6 is specific for mitochondria. To rule out the possibility of DiOC6 staining other negatively charged organelles, we performed confocal imaging analysis. At 20nM concentration, DiOC6 overlaps with mitochondrial dye Mitotracker Deep Red (Figs. 1A, S1, Supplemental video 1). Image analysis indicated that low dose DiOC6 and Mitotracker Deep Red co-localize (Table S1). Therefore, DiOC6 was used in subsequent $\Delta\Psi_m$ analysis. Figures 1B and C indicate the gating strategy for measuring T cell $\Delta\Psi_m$ from PBMC and enriched T cells, respectively. Figure 1C also indicates the analysis of apoptosis by staining with Annexin-V and Propidium Iodide.

T cells from patients with type 1 diabetes exhibit MHP. To study T cell mitochondrial function, we first analyzed $\Delta\Psi_m$ in T cells from fresh PBMC by flow cytometric analysis. When compared to healthy controls, the T cells of patients with type 1 diabetes exhibited significant MHP (Fig. 2A–C). In individuals with T cell MHP, the phenotype was detected in CD4⁺ (Fig. 2A; $P < 0.05$), CD8⁺ (Fig. 2B; $P < 0.0001$), and total CD3⁺ (Fig. 2C; $P = 0.001$) T cell populations. These data suggested that MHP was a general characteristic of T cells in patients with type 1 diabetes.

To determine if T cell MHP was associated with activation or the transition from a naïve to differentiated T cell phenotype, we initiated a second phase of the study and recruited an additional 107 participants (Table 1). We analyzed $\Delta\Psi_m$ in each subset of T cells by co-staining PBMC with markers to identify naïve and memory T cell compartments as well as markers of T cell activation status. A total of 10 groups of lymphocytes, including 9 subsets of T cells were defined. Individuals with T cell MHP exhibited this phenotype globally across naïve (CD45RA⁺ CD45RO⁻) and memory (CD45RO⁺ CD45RA⁻) subgroups of both CD4⁺ and CD8⁺ T cells, as well as conventional (CD127⁺ CD25⁻) and regulatory (CD127⁻ CD25⁺) CD4⁺ T cell subsets. Pairwise correlation analysis failed to detect strong associations between the $\Delta\Psi_m$ and any of the nine T cell subsets analyzed (See Supplementary Table S1). Further, T cell MHP was not associated with any change in resting viability, altogether indicating that when MHP was present, it was consistently observed in all T cell subsets regardless of their activation status. In sum, MHP appeared to be a phenotype that was intrinsic to all T cell subsets.

Given that MHP in subsets of subjects was consistent among all T cell subsets regardless of their activation status, we further analyzed $\Delta\Psi_m$ using enriched total T cells in an independent cohort of research participants (Phase 3; Table 1). We were able to confirm the link between T cell MHP and type 1 diabetes (Fig. 2D; $P = 0.018$) identified in phases 1 of this study. To further analyze the effect of hyperglycemia on T cell $\Delta\Psi_m$, a group of patients with type 2 diabetes ($n = 20$) was included in this cohort (Phase 3; Table 1). The HbA1c level of the type 1 diabetes group was 7.9 ± 2.1 (% Mean \pm SD) while that of the type 2 diabetes group was 7.8 ± 2.6 . T cell $\Delta\Psi_m$ from type 2 diabetes patients was indistinguishable from controls (Fig. 2D) and significantly lower than the type 1 diabetes group ($P = 0.0005$). When analyzing all three phases of the study, no correlations were detected between: (1) $\Delta\Psi_m$ and age (Fig. 2E), (2) $\Delta\Psi_m$ and HbA1c levels (Fig. 2F), (3) $\Delta\Psi_m$ and duration of diabetes (See Supplementary Fig. S2A), or (4) $\Delta\Psi_m$ and glucose levels at blood sampling (See Supplementary Fig. S2B). Together, these data suggest that MHP is intrinsic to T cells from patients with type 1 diabetes and is not a consequence of abnormal glucose control.

MHP is associated with functional changes in T cells after activation. Cryopreserved PBMC samples from Phase 1 individuals (Table 1 and Fig. 1A–C) were chosen, including a total of 6 with MHP (5 type 1 diabetes, 1 control) and 26 with normal $\Delta\Psi_m$ (10 type 1 diabetes and 16 controls; Fig. 3A) to determine the effect of MHP on T cell function. Cells were stimulated *in vitro* with plate-bound anti-CD3, soluble anti-CD28 for 72 hours. Using Cell Trace Violet, we observed that cell proliferation was not significantly different when comparing MHP versus normal $\Delta\Psi_m$ groups ($P = 0.145$). However, intracellular IFN γ staining indicated that CD4⁺ T cells with MHP exhibited elevated IFN γ production when compared to T cells without MHP (Fig. 3B; $P = 0.02$). These data suggest an altered pro-inflammatory T cell effector response is associated with MHP.

T cell mitochondria respond to TCR stimulation by increasing mass, $\Delta\Psi_m$, and ROS generation¹⁵, and mitochondrial ROS is essential for signal transduction during T cell activation^{7,16}. To study if abnormal mitochondrial responses to T cell activation are linked to T cell dysfunction in type 1 diabetes, total T cells were enriched from fresh peripheral blood and stimulated *in vitro* with plate-bound anti-CD3 and anti-CD28 for 24 hours. Activation-induced IFN γ , detected in the supernatant of anti-CD3/anti-CD28 stimulated cells, was positively correlated with mtROS production (Fig. 3C). Although we did not observe an increase of activation-induced $\Delta\Psi_m$ in all T cell samples, the increase in $\Delta\Psi_m$ correlated with mtROS production (Fig. 3D). These data linked the type 1 diabetes-associated altered activation-induced mitochondrial response with altered effector T cell cytokine production.

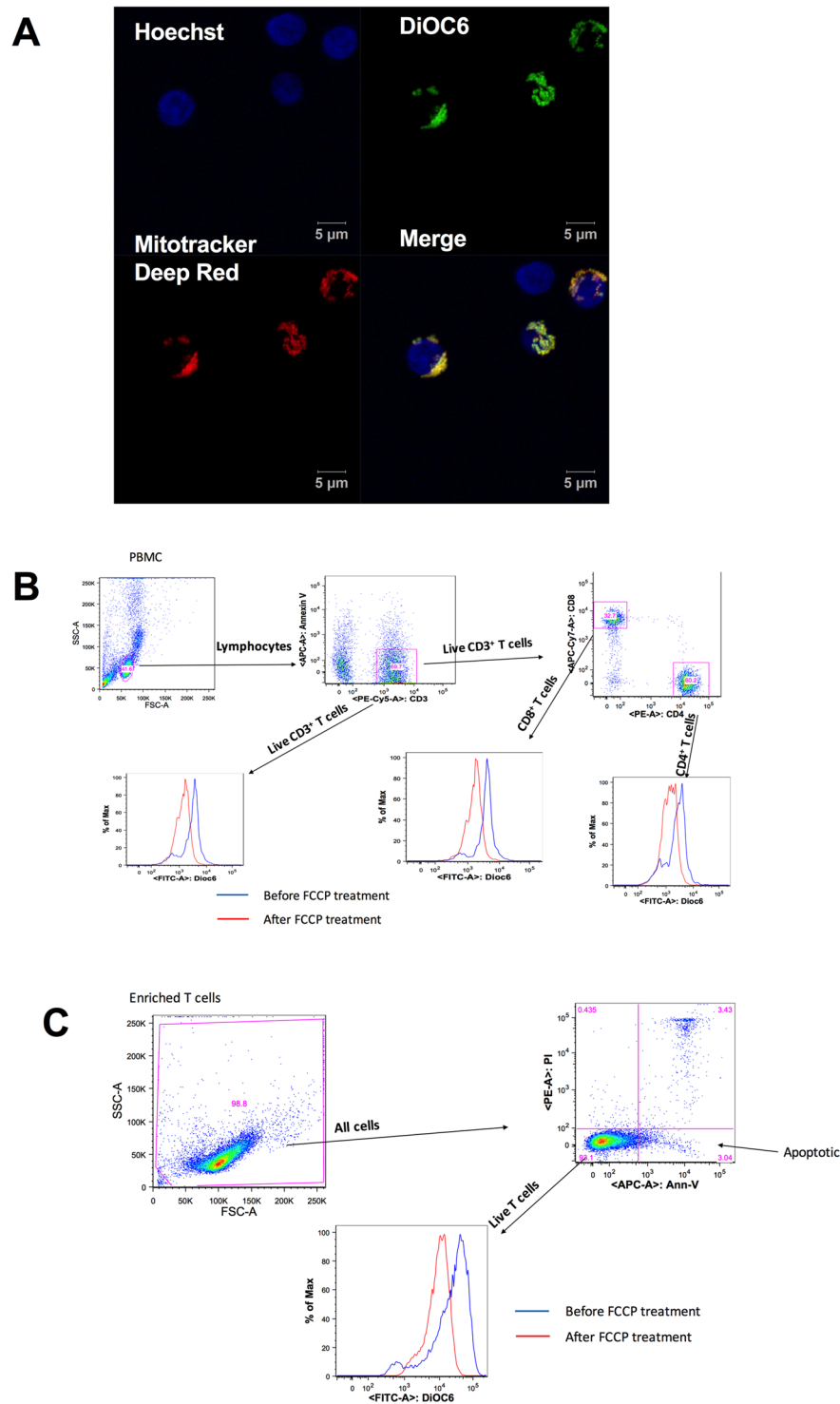


Figure 1. Staining and gating strategies for $\Delta\Psi_m$ measurement. **(A)** Confocal image shows co-localization of low dose DiOC6 (20nM) and Mitotracker Deep Red in enriched human T cells. Green: DiOC6; Red: Mitotracker Deep-Red; Blue: Hoechst 33258. **(B)** Gating strategy for measuring T cell $\Delta\Psi_m$ in human PBMC. **(C)** Gating strategy for measuring $\Delta\Psi_m$ and apoptosis in enriched human T cells. $\Delta\Psi_m$ was expressed as MFI of DiOC6 that was corrected with the value from the same sample after FCCP treatment as mentioned in method session.

Lower basal cellular ATP levels observed in T cells of type 1 diabetes subjects. A major function of mitochondria is the generation of cellular ATP. Although the traditional concept holds that upon activation, T cells utilize glycolysis for energy production (Warburg effect¹⁷), ATP from mitochondrial oxidative

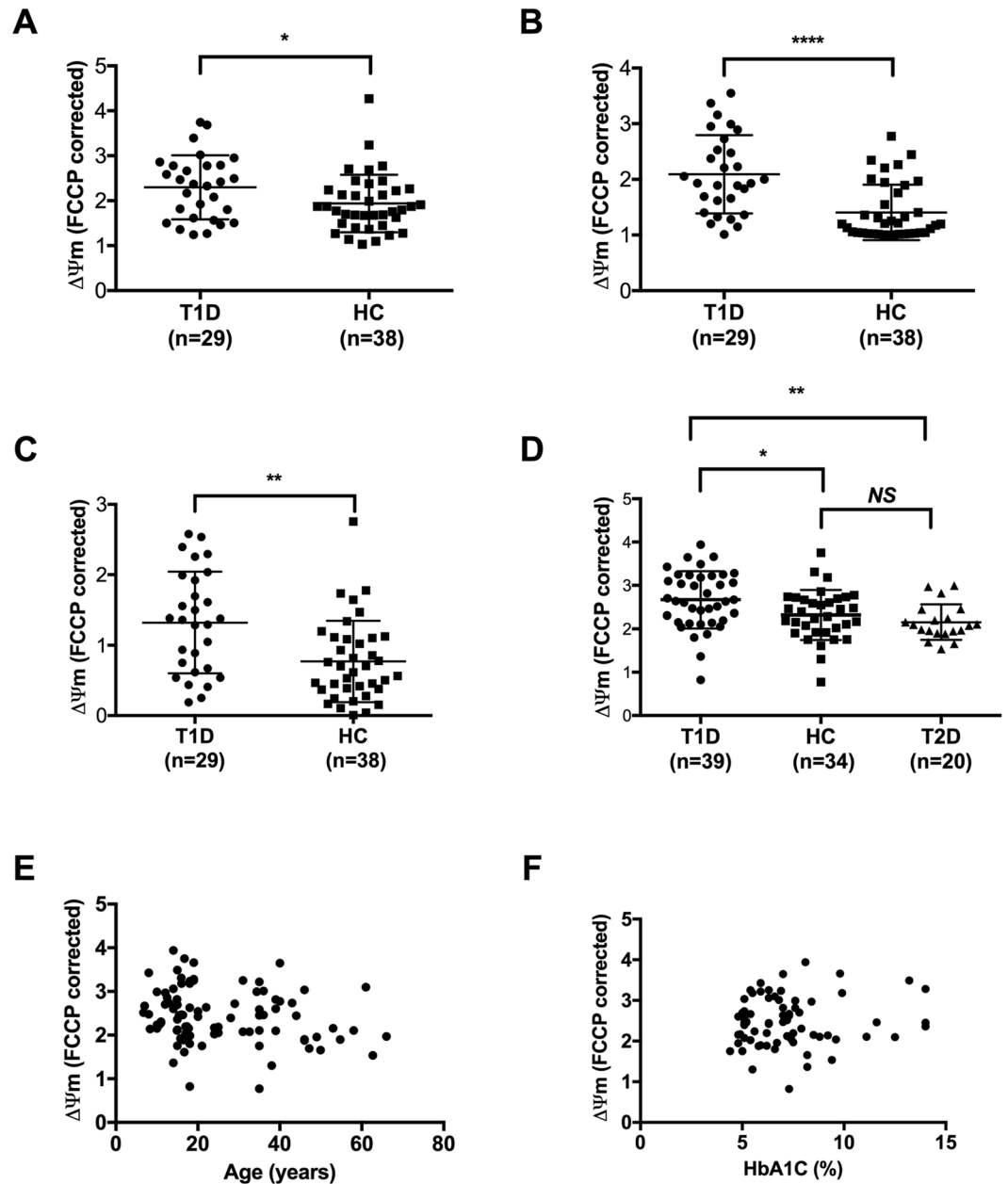


Figure 2. T cells from patients with type 1 diabetes exhibited MHP. T cells from peripheral blood of type 1 diabetes patients (T1D; $n = 29$) exhibited a higher mitochondrial membrane potential ($\Delta\Psi_m$) when compared to T cells from healthy controls (HC; $n = 38$) in (A) $CD4^+$, (B) $CD8^+$ and (C) $CD3^+$ subsets; (D) In an independent cohort, enriched total T cells from fresh blood of T1D patients ($n = 39$) showed higher $\Delta\Psi_m$ when compared to HC individuals ($n = 34$) or patients with type 2 diabetes ($n = 20$). T cell $\Delta\Psi_m$ was not correlated with (E) age or (F) HbA1c level. * $P < 0.05$, ** $P < 0.005$, **** $P < 0.001$. Mann-Whitney test.

phosphorylation (OXPHOS) is also required during T cell activation and differentiation¹⁸. Mitochondrial ATP is thought to be important for events that initiate T cell activation. We therefore monitored T cell ATP content after polyclonal stimulation with activating anti-CD3 and anti-CD28 antibodies and used isotype antibody-treated samples to assess basal ATP production. When compared to healthy controls, T cells purified from subjects with type 1 diabetes exhibited significantly reduced cellular ATP content prior to activation (Fig. 4A; $P = 0.023$) suggesting compromised mitochondrial function of these cells. Activation *in vitro* for 24 hours led to an increase of ATP in cells from both patient and control samples. This was not surprising since aerobic glycolysis is the main metabolic pathway after T cell activation¹⁹. During activation, increased ATP production via glycolysis may be able to facilitate activation-induced signal transduction and downstream cytokine production.

NO is a regulator of mitochondrial biogenesis²⁰. At low concentrations, this molecule can inhibit mitochondrial complex IV by competing for oxygen. At higher concentrations, NO can damage electron transport complexes and members of the TCA cycle²¹. NO has been found to be the essential cause of T cell mitochondrial

Phase	Participant Group	n	Age [Years(Medianrange)]	Gender [% Female]	Disease Duration [Years (Median, range)]	HbA1C [%]
1		67				
	Type 1 diabetes	29	14, 9–27	55%	5.6, 0.1–18.6	7.1–14.6
	Healthy control	38	16, 7–38	42%	N/A	ND
2		107				
	Type 1 diabetes	25	12, 4–60	44%	2.67, 0.08–18	ND
	Healthy Control	21	33.5, 19–51	52%	N/A	ND
	Type 2 diabetes	1	45	100%		ND
	1st Degree Relative	53	30, 4–56	60%		
	2nd Degree Relative	7	60, 50–66	86%		
3		93				
	Type 1 diabetes	39	18, 6.8–61	51%	8, 0.08–35.1	9.9–14
	Healthy control	34	22.5, 7–53	62%		ND
	Type 2 diabetes	20	34.5, 10.6–66	65%	3.25, 0.08–22	4.8–14
Functional Studies		137				
	All Phase 3	93				
	Healthy control	3	44, 22–45	67%		ND
	1st Degree Relative	40	32.5, 8–61	48%		ND
	Type 2 diabetes	1		0%		ND

Table 1. Research Subjects Participating in the Three Study Phases.

dysfunction in SLE patients¹². We analyzed T cell NO production 24 hours after polyclonal activation *in vitro* but did not detect significant differences between type 1 diabetes and controls in activation-induced NO production (See Supplementary Fig. S3). Lack of differences in NO production from T cells in type 1 diabetes and controls suggests that, unlike in the case of SLE, the mitochondrial dysfunction in type 1 diabetes is not linked to elevated NO production.

T cell MHP does not change activation-induced T cell apoptosis. There was no difference in T cell activation-induced cell death/apoptosis (AICD) between type 1 diabetes and control subjects (Fig. 4B). Similarly, when segregated into MHP group (n = 7: 5 type 1 diabetes, 2 controls) and normal $\Delta\Psi_m$ group (n = 65: 33 type 1 diabetes and 32 controls), there was no difference in T cell AICD (Fig. 4C). AICD was not correlated with $\Delta\Psi_m$ value (Fig. 4D), nor were changes detected in activation-induced necrosis.

T cell MHP is not associated with changes in glycolysis. Samples from a subset of participants (n = 29, including 11 patients with type 1 diabetes, 4 healthy controls, 13 relatives, and a patient with type 2 diabetes) in phase 2 were subjected to glycolysis detection with an Seahorse XF24 extracellular flux analyzer. No correlation was detected between T cell MHP and glycolysis (Fig. S4).

Discussion

Mitochondrial metabolic activity plays a central role in regulating T cell activation, proliferation, and programmed cell death⁴. During T cell activation, mitochondria are recruited to under the immunological synapse where they participate in TCR signaling and T cell proliferation by regulating ATP synthesis, local calcium concentrations^{5, 22, 23}, and generate ROS^{7, 16}. The roles of metabolic control and mitochondria activity in T cell function have drawn great attention in recent years. Metabolic control of T cell activity may play a critical role in determining autoimmune disease progression through maintenance of peripheral immune tolerance¹⁸.

In this study, we observed for the first time that T cells from patients with type 1 diabetes exhibit MHP. When MHP was present it was detected in all subsets of T cells regardless of activation status and was not correlated with disease duration or HbA1c level. In addition, MHP was not observed in T cells from patients with type 2 diabetes, whose metabolic status was comparable to the type 1 diabetes group based on HbA1c levels. These data suggest that MHP is an intrinsic T cell defect rather than a consequence of disease status, metabolic control, or recent antigen exposure and activation state. Although DiOC6 can stain other negatively charged membranous structures inside of cells, such as the endoplasmic reticulum, at lower concentrations DiOC6 is specific to mitochondria^{24, 25}. In this study, we used a low DiOC6 concentration (20 nM as previously published^{15, 26}) to assess $\Delta\Psi_m$ in lymphocytes. In addition, using confocal images, we demonstrate that 20nM DiOC6 in combination with the mitochondrial-specific dye Mitotracker-Deep Red are co-localized in both BetaLox 5 cells, with clear mitochondrial structure, and enriched human T cells (Fig. 1A, Supplemental Figure S1, Supplemental video S1, and Table S2 (Co-localization analysis)).

Upon TCR stimulation, signaling pathways lead to activation of transcription factors and the production of inflammatory cytokines^{27, 28}. The T_H1 lineage, characterized by high levels of IFN γ production, is considered an important component of type 1 diabetes pathogenesis²⁹. Our finding that upon TCR stimulation, CD4⁺ T

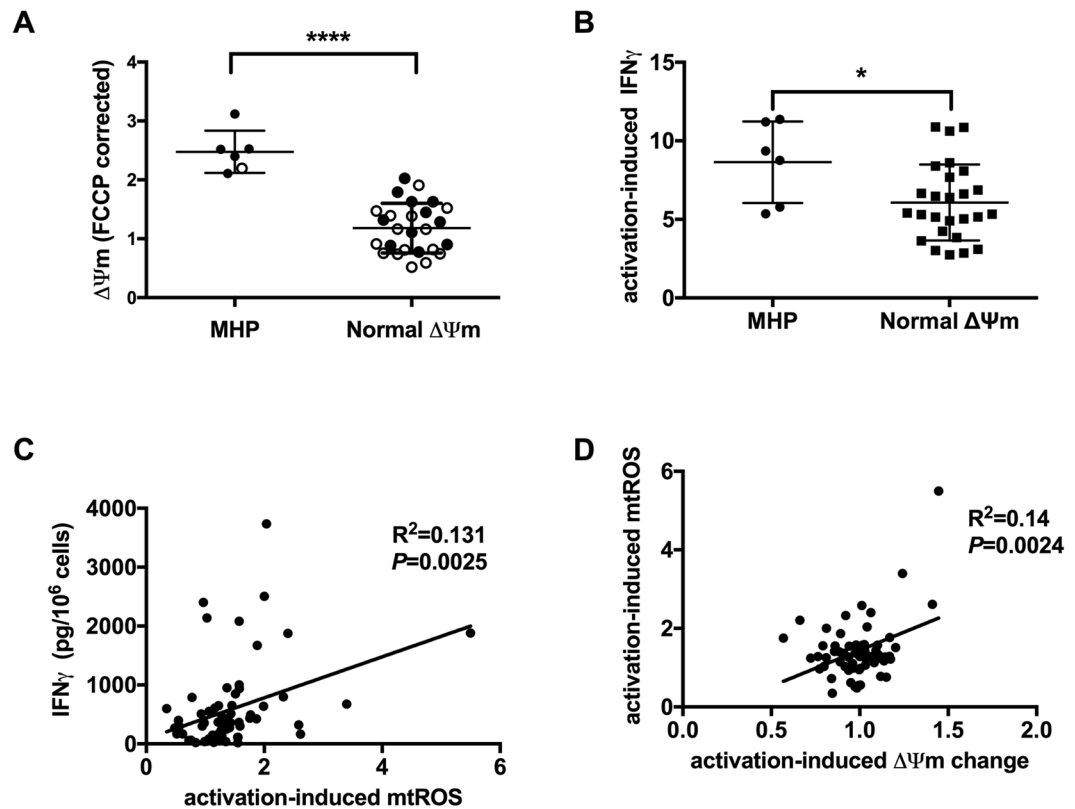


Figure 3. T cell MHP is associated with functional changes upon activation. (A) T cell $\Delta\Psi_m$ of individuals whose cryopreserved PBMC samples were selected for *in vitro* activation. Black dot: type 1 diabetes patients. Open circles: healthy controls. (B) CD4^+ T cells from cryopreserved PBMC of individuals with MHP ($n=6$, including 5 type 1 diabetes patients and 1 healthy control) show higher intracellular $\text{IFN}\gamma$ staining after 72-hour stimulation with plate-bound anti-CD3 and anti-CD28, when compared to cells from individuals without MHP ($n=26$, including 10 type 1 diabetes patients and 16 healthy controls). (C) Mitochondria-specific ROS produced by enriched total T cells after stimulating by plate-bound anti-CD3 and anti-CD28 for 24 hours, is correlated with the amount of $\text{IFN}\gamma$ secreted in the supernatant. (D) Activation-induced change of $\Delta\Psi_m$ is positively correlated with mt-specific ROS production after 24-hour stimulation *in vitro*. * $P < 0.05$, **** $P < 0.0001$, Mann-Whitney test (A and B). Linear regression (C and D).

cells with MHP secrete greater amounts of $\text{IFN}\gamma$ suggests that MHP is linked to differentiation of CD4^+ T cells toward the $\text{T}_{\text{H}}1$ lineage³⁰. While ROS and cytokines participate in the pathogenesis of type 1 diabetes^{31–33}, a recent study using animal models has shown that mitochondria metabolism and ROS production from mitochondrial complex III is required for antigen-specific T cell activation⁷. Moreover, increasing mitochondrial production of hydrogen peroxide by overexpressing superoxide dismutase 2 (SOD2 or MnSOD) has been shown to enhance TCR signaling. In our study, we evaluated mtROS induction by TCR stimulation in combination with co-stimulation. Using enriched total T cells, after a 24-hour stimulation with plate-bound anti-CD3 and anti-CD28, we observed that activation-induced mtROS generation was correlated with $\text{IFN}\gamma$ production. Hence, we hypothesize that dysfunctional mitochondria generate more ROS and further, that increased levels of ROS can stimulate transcription factors which facilitate production of inflammatory cytokines⁶.

T cell MHP has been previously observed in human autoimmunity: in SLE patients, the presence of MHP was linked to lower ATP production and a switch of T cell death from apoptosis to necrosis²⁶. Our observation that T cells from type 1 diabetes patients show lower cellular ATP content in a quiescent state is consistent with T cells from SLE being ATP-depleted. However, while in SLE patients, T cell MHP is linked to decreased T cell viability due to elevated T cell necrosis^{8–10}, we did not observe any changes of T cell necrosis or apoptosis in type 1 diabetes patients or individuals with T cell MHP.

An additional difference between T cell MHP in type 1 diabetes and SLE is the participation of NO in SLE. In SLE, T cell MHP is highly correlated with NO levels, while in type 1 diabetes we did not observe a link between MHP and NO. NO is a regulator of mitochondrial biogenesis and function. At low concentrations, NO reversibly inhibits mitochondrial cytochrome c oxidase (OXPHOS Complex IV) by competing with oxygen at the active site of the enzyme³⁴. At high concentrations, NO can react with superoxide to produce peroxynitrite (ONOO^-), which can react with and inactivate multiple mitochondrial complexes (I, II, III, IV), the ATP synthetase (ATPase), creatine kinase, as well as aconitase. Further, ONOO^- stimulates proton leak through the mitochondrial inner membrane³⁵. NO may also facilitate generation of Nitrosothiols (RSNO) that can also inhibit

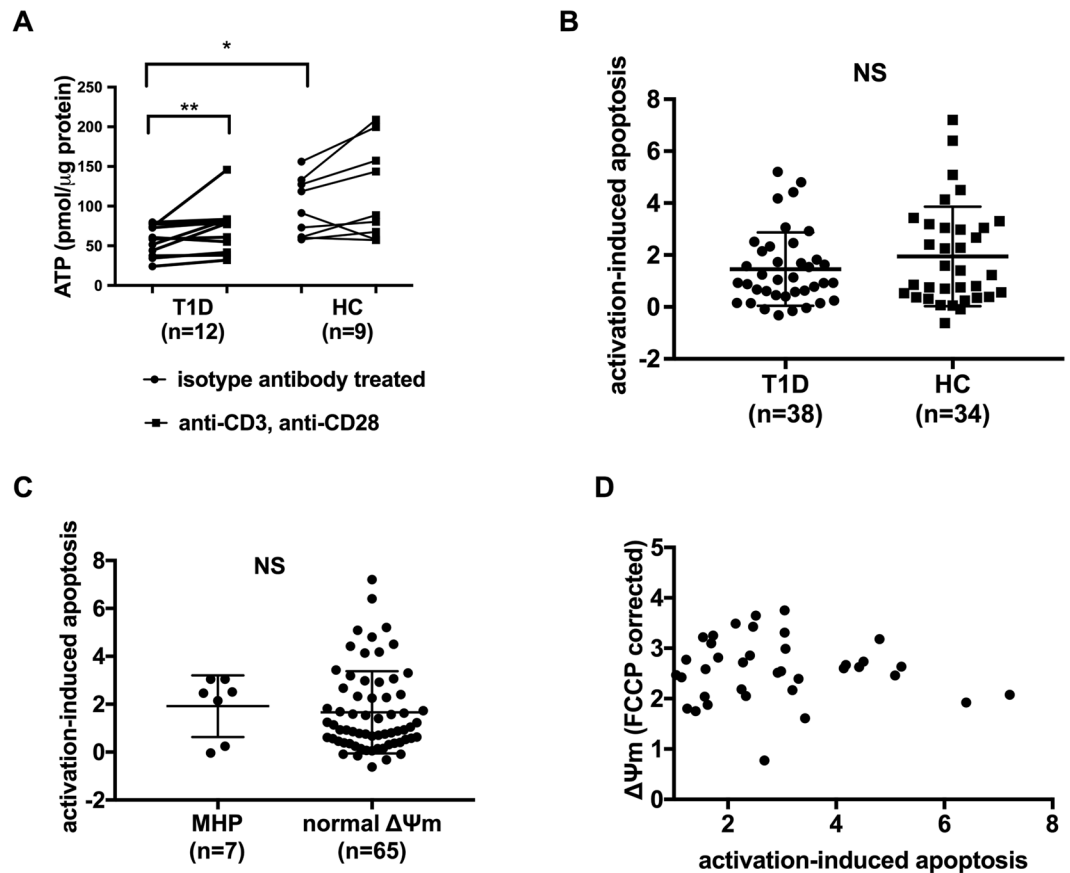


Figure 4. Activation-induced ATP and cell death. (A) T cells from type 1 diabetes patients (T1D) have lower basal cellular ATP content compare to healthy controls (HC) but cellular ATP was significantly increased after *in vitro* activation. Enriched total T cells were stimulated *in vitro* with plate-bound anti-CD3 and anti-CD28 or isotype antibodies for 24 hours. ATP content was detected in cell lysate and corrected by protein amount. The trend remains that T cells from type 1 diabetes patients have lower ATP content even though *in vitro* activation induces a significant increase of ATP in this group. (B) T cells from T1D patients and HC showed the same level of activation-induced apoptosis. After 24-hour activation with plate-bound anti-CD3 and anti-CD28, T cell apoptosis was identified by staining with Annexin-V and Propidium Iodide. Activation-induced apoptosis was calculated as mentioned in method session. (C) T cells with MHP showed the same activation-induced apoptosis as normal $\Delta\Psi_m$ T cells. (D) Activation-induced apoptosis was not correlated with T cell $\Delta\Psi_m$. * $P < 0.05$, unpaired t test with Welch's correction. ** $P < 0.01$ Wilcoxon matched pair test for (A) and Mann-Whitney test for (B).

mitochondrial complex I³⁵. NO has been found to be the essential cause of T cell mitochondrial dysfunction in human SLE¹². We did not observe an increase of NO in T cells from type 1 diabetes patients after activation. The difference between the previous observations in SLE patients and our study may be related to the observation that the increased NO in SLE patients originated from monocytes as opposed to T cells, although the same group also reported that NO produced from T cells is increased after activation¹².

Under normal conditions, TCR stimulation induces a transient decrease of mitochondrial membrane potential within 30 seconds, which is synchronized with a spike in the ATP concentration³⁶ that is required for mediating signaling events. Activated T cells then experience a reversible mitochondrial hyperpolarization¹⁰. That is accompanied by an induction of glycolysis for energy production (Warburg effect¹⁷) as well as activation of the pentose phosphate pathway (PPP)³⁷ for biosynthesis. PPP is regulated by a key enzyme transaldolase³⁸. In addition to producing ribose-5 phosphate for nucleic acid synthesis and cell proliferation, PPP also generates NADPH from NADH by the enzyme G6PD and 6-phosphogluconate dehydrogenase (PGD). NADPH is an important reducing agent that reduces glutathione^{37,39}. These changes in PPP are accompanied the reversible MHP in activated T cells. In autoimmune settings like SLE¹⁰ and type 1 diabetes, the T cell MHP is constant, and our data indicate that in type 1 diabetes, MHP is not restricted to activated T cell subsets only. Although we have not yet examined PPP in these T cells, the persistent MHP in T cells of type 1 diabetes is not likely the result of a PPP associated increase of NADPH and glutathione reduction. On the other hand, the fact that T cell MHP is not associated with glycolytic changes in these cells (Fig. 4S) further suggests that MHP in type 1 diabetes is distinct from activation-induced reversible MHP found in T cells from controls¹⁰. Our data suggest that the original cause of T cell MHP in type 1 diabetes patients is different from that observed in SLE patients. It is more likely that MHP

observed in the T cells of patients with type 1 diabetes results from an intrinsic abnormality of the mitochondria that may arise from the genetic predisposition that is linked to T cell dysregulation in type 1 diabetes.

Indeed, T cell MHP is a novel finding in human type 1 diabetes. MHP is associated with altered T cell response following TCR ligation and co-stimulation. Dysregulated mitochondria in T cells could play a role in disturbances in both central and peripheral mechanisms of immune tolerance. These data demonstrate that altered lymphocyte mitochondrial function and metabolism within type 1 diabetes represent a significant contributor to autoimmune pathogenesis and may constitute a novel therapeutic target for restoring immune regulation. It is worth noting that, although our study indicates that MHP is general to all T cell subsets in type 1 diabetes, it does not indicate that all of these T cell subsets have the same metabolic program. Indeed, it has been well known that different T cell subsets have distinct metabolism characteristics. Future investigations are necessary to study how each T cell subset metabolism changes affect immune balance in the context of type 1 diabetes.

Methods

Research subjects. All participants in this three-stage study were enrolled from University of Florida Diabetes Institute clinical network. In the first phase of the study, 38 healthy controls and 29 patients with type 1 diabetes were recruited (Table 1). An extended second-phase study was also conducted to further characterize the activation status of T cells with MHP by enrolling 107 individuals (Table 1). The third phase of this study enrolled 93 individuals to confirm our original observation of MHP as a characteristic of T cells from patients with type 1 diabetes. Samples of all individuals from phase 3 and an additional 44 were proceeded for functional studies (Table 1).

Study Approval. All studies described within were consented in accordance with an approved study reviewed by the Institutional Review Board of the University of Florida. Written informed consent was received from each participant prior to inclusion in the study.

Sample preparation. Peripheral blood samples were collected in heparin containing vacutainer tubes (BD Biosciences). For the assays in phase 1 and phase 2, PBMC were isolated within 24 hours of sample collection by first dilute whole blood with 1X D-PBS (no glucose) at 1:1 ratio followed by ficoll gradient⁴⁰. These PBMCs were stained and analyzed by flow cytometry. For the phase 3 immunophenotyping and functional studies, total T cells were enriched using a RosetteSep T cell enrichment kit (Stemcell Technologies).

T cell $\Delta\Psi_m$ analysis. In the first-phase of the study, fresh PBMC were stained with the T cell surface markers anti-CD3 (Clone UCHT1, BioLegend, #300409), anti-CD4 (Clone RPA-T4, BioLegend, #300507), and anti-CD8 (Clone HIT8a, Biolegend, #300925) for 30 minutes at 4°C, washed, and then stained for $\Delta\Psi_m$ with 3,3'-Dihexyloxycarbocyanine Iodide (DiOC₆; 20nM), a cell-permeable, green-fluorescent, lipophilic dye for 15 minutes at 37°C. Cells were then washed, Annexin-V (Invitrogen) added, and analyzed using a BD LSR Fortessa flow cytometer. Dead cells were excluded by gating out the Annexin-V positive subset. This 5-color panel was used to detect T cells $\Delta\Psi_m$. $\Delta\Psi_m$ was expressed as Mean Fluorescence Intensity (MFI) of DiOC₆ for each gated T cell subset. To diminish instrumental bias, baseline $\Delta\Psi_m$ was obtained by treating each sample with Carbonyl cyanide-4- (trifluoromethoxy) phenylhydrazone (FCCP, 1 μ M), a mitochondrial uncoupler, for 10 minutes, and the baseline MFI was used to correct for the corresponding DiOC₆ reading. In the second phase of the study, fresh PBMC were stained with a 9-color panel including the T cell surface markers anti-CD3 (Clone UCHT1, Biolegend, #300424), anti-CD4 (Clone RPA-T4, BD Biosciences, #558116), and anti-CD8 (Clone SK1, Biolegend, #344714), plus the activation markers CD45RA (Clone HI100, BD Biosciences, #560675), CD45RO (Clone UCHL1, Biolegend, #304222), CD127 (Clone HIL-7R-M21, BD Biosciences, 557938) and CD25 (Clone BC96, Biolegend, #302610). Fluorescence minus one (FMO) control was setup for CD25 gating accuracy. Dead cells were gated out using LIVE/DEAD[®] Fixable Yellow Dead Cell Stain Kit (Invitrogen). $\Delta\Psi_m$ was detected as described above. All the above steps were performed using HBSS with no addition of glucose. For the second phase, the cytometer instrumental settings were adjusted to work with the 9-color panel; therefore, the results of this phase were not combined with results from phase 1. Instead, they were analyzed independently.

In the third phase of the study, enriched total T cells were stained for $\Delta\Psi_m$ using DiOC₆ in phenol red-free complete RPMI (Glucose concentration 2 G/L) for 15 minutes at 37°C, washed with and re-suspended in Annexin-V binding buffer (10 mM HEPES, 140 mM NaCl, 2.5 mM CaCl₂, 2% FBS, no glucose, PH 7.2). Annexin-V and PI were added before running on flow cytometer. To equalize the effect of environment on mitochondrial function, in each phase of the study, samples from controls and patients were prepared the same way, including reagents concentration, staining time, incubation temperature and duration, washing process, speed, temperature, as well as force and duration of centrifugation. Flow cytometer data were analyzed using Flowjo software (Tree Star Inc. Version 8.8.7-9.7.7).

T cell activation *in vitro* (72-hour stimulation). Samples with MHP ($\Delta\Psi_m$ greater than median + 1SD) and normal $\Delta\Psi_m$ ($\Delta\Psi_m$ lower than median + 1SD) were selected from Phases 1 and 3. Twenty-four well plates were coated with crosslinking anti-mouse IgG Fab2 (Jackson Immuno Research) at a final concentration of 1.25 μ g/mL in sterile PBS at 4°C for 16 hours. Crosslinking Fab2 was removed, and then wells were rinsed once with sterile PBS. Either anti-CD3 (OKT3, Biolegend, #317315) or isotype control antibody (IgG2a k isotype ctrl, Biolegend, #40022477) was added at final concentration 1.25 μ g/mL and plates were incubated at 37°C for 3 hours. Coating antibodies were removed and wells rinsed with PBS once before adding PBMC.

Frozen PBMC samples were selected from individuals that participated in phase 1 and included individuals with MHP (n = 6) and those without MHP (n = 26). Samples were thawed, loaded with CellTrace Violet (Life Technologies), and seeded in coated plates at a density of 10⁶ cells per well in 1mL complete RPMI. Soluble

anti-CD28 (BD Pharmingen, #555725) or isotype control IgG1 k antibody (ebioscience, #16-4714-85) was added at final concentration 2.5 µg/mL. Cells were stimulated for 72 hours. Golgistop was added for the final 4 hours. After stimulation, cells were stained with LIVE/DEAD™ Fixable Yellow Dead Cell Stain Kit (Life Technologies Ref# L34959), then stained for T cell surface markers, anti-CD3 (Clone OKT3, Biolegend #317318), anti-CD4 (Clone RPA-T4, BD Pharmingen #555347), anti-CD8 (Clone B9.11, Beckman Coulter #IM0451U). Subsequently, cells were fixed and permeabilized with BD Cytfix/Cytoperm Kit (BD Biosciences), and stained for intracellular IFN γ (Biolegend #502528). Samples were analyzed by flow cytometry. Dead cells were gated out using Live-Dead yellow positivity. Cell proliferation was analyzed by dilution of CellTrace Violet using Flowjo software to calculate number of peaks, percent divided, proliferation and division indices. T cell IFN γ MFI was assessed under activating conditions (MFI_{Act}) as well as in samples treated with isotype antibodies (MFI_{Iso}), and activation-induced IFN γ was calculated as $(MFI_{Act} - MFI_{Iso}) / MFI_{Iso}$.

T cell activation-induced mitochondrial functional changes (T cells were activated for 24 hours *in vitro* for this purpose).

Total T cells were enriched from fresh peripheral blood using the RosetteSep Human T Cell Enrichment Cocktail (Stemcell Technologies, #15021). Twelve-well plates were coated with anti-CD3 (Biolegend, #317315, clone OKT3, final concentration 10 µg/ml in PBS) or mouse IgG2a, k isotype control (BioLegend, #400224, clone MOPC-173, final concentration 10 µg/ml in PBS) for 3 hours at 37 °C. Coated wells were then rinsed once with PBS and enriched T cells were seeded at 1×10^6 cells/well. Anti-CD28 (BD Biosciences, #555725, final concentration 20 µg/ml) was added to anti-CD3 coated wells, and mouse IgG k isotype control (eBiosciences, #16-4714-85, final concentration 20 µg/ml) was added to isotype-antibody coated wells. Cells were incubated at 37 °C for 24 hours. After activation, T cell $\Delta\Psi_m$ was analyzed by staining with the fluorescent probe DiOC₆ and corrected with FCCP as mentioned above. mtROS production was detected by staining with the fluorescent mitochondrial specific ROS indicator probe MitoSox-Red (Life technologies, #M36008, 5 µM) at 37 °C for 15 minutes. Cellular nitric oxide (NO) production was detected by staining with DAF-FM Diacetate (Life technologies, #D23844, final concentration 2 µM) at 37 °C for 15 minutes. Dead cells and apoptotic cells were excluded by staining with the combination of Annexin-V and PI or 7AAD (BD Biosciences). Data were recorded using a BD LSR Fortessa cytometer. Cellular ATP contents were detected using ATP determination Kit (Life Technologies, # 1577278), read on a BioTek Synergy 2 Multi-Mode Reader, and corrected for protein content measured using the BCA assay (Pierce). Cytokines in culture supernatants were determined using ELISA according to manufacturer recommendations (BD Biosciences). Activation-induced mtROS was calculated as MFI_{Act} / MFI_{Iso} of MitoSox-Red staining. Activation induced $\Delta\Psi_m$ change was calculated as the ratio MFI_{Act} / MFI_{Iso} of DiOC₆ staining. Activation induced NO production was calculated as MFI_{Act} / MFI_{Iso} of DAF-FM Diacetate staining. Activation-induced apoptosis was calculated as the difference in percent Annexin-V positive PI negative apoptotic cells (%Apo) between activating antibody and isotype antibody treated conditions, divided by that of the isotype treated sample $[(\%Apo_{Act} - \%Apo_{Iso}) / \%Apo_{Iso}]$. Necrotic cells were gated on PI-positive population (%Necro) and activation-induced necrosis was calculated as $[(\%Necro_{Act} - \%Necro_{Iso}) / \%Necro_{Iso}]$.

Glycolysis measurement. Enriched T cells were seeded in a 24-well XF Extracellular Flux Analyzer plate at 5×10^5 cells/well in triplicates. Real-time extracellular acidification rates (ECAR) were recorded using an XF Extracellular Flux Analyzer (Fig. S4A). Activating antibodies or respiratory inhibitors were injected at time points as shown in Figure S4A. (a) AntiCD3 (2 µg/mL) plus antiCD28 (1 µg/mL), or isotype antibodies at the same concentrations, (b) ATP synthase inhibitor Oligomycin (12.6 µM), (c) uncoupler Carbonyl cyanide 4-(trifluoromethoxy) phenylhydrazone (FCCP, 1 mM), (d) glycolysis inhibitor 2-DG (44.6 mM), mitochondrial complex I inhibitor Rotenone (1 mM) and mitochondrial complex III inhibitor antimycin A (1 mM). All the above are final concentrations.

Confocal Microscopy. Human beta cell line BetaLox5 cells^{41, 42} were seeded in chambered glass 1 day prior to staining and imaging. Enriched T cells were stained in Eppendorf tubes before seeding in chambered glass. Cells were stained with DiOC₆ 20 nM, MitoTracker™ Deep Red FM (Thermo Fisher, M22426) 10 nM, and Hoechst 33258 2 µg/mL for 20 minutes at 37 °C. Images were taken using Zeiss 710 Laser Scanning Confocal Microscope. BetaLox5 image was taken with 40X dry objective with a 2.5X digital zoom. T cell images were taken with a 63X oil objective with a 3X digital zoom. 3D image of T cells was processed as video (Supplemental video) and as maximum intensity projection (Fig. 1A). Colocalization parameters were calculated using Zeiss Zen2.1 software (Carl Zeiss).

Statistics. Data were analyzed using GraphPad Prism (Version 6.0g, GraphPad Software, Inc) and JMP 7 (SAS Institute Inc). One-way ANOVA with Bonferroni post-hoc corrections was used for multiple comparisons, and unpaired t-test with Welch's correction was used when comparing two groups. Correlations were conducted by Spearman analysis or Multivariate correlation analysis. For paired samples, stimulated and isotype control treated conditions were compared via Wilcoxon test. Non-parametric analyses were conducted by Mann-Whitney tests with $p < 0.05$ deemed significant.

Data availability. The datasets generated during and/or analyzed during the current study are available from the corresponding author on reasonable request.

Prior Presentations. Parts of this study were presented in abstract form at 12th Annual Meeting of the Federation of Clinical Immunology Societies, Vancouver, Canada, June 2012, and 73rd American Diabetes Association Scientific Session, Chicago, June 2013, Immunology of Diabetes Society 14th International Congress, Munich, Germany, April 2015, and American Diabetes Association Scientific Session, New Orleans, June 2016.

References

- Atkinson, M. A. The pathogenesis and natural history of type 1 diabetes. *Cold Spring Harb Perspect Med* **2**, doi:10.1101/cshperspect.a007641 (2012).
- van der Windt, G. J. & Pearce, E. L. Metabolic switching and fuel choice during T-cell differentiation and memory development. *Immunol Rev* **249**, 27–42, doi:10.1111/j.1600-065X.2012.01150.x (2012).
- Buck, M. D., O'Sullivan, D. & Pearce, E. L. T cell metabolism drives immunity. *J Exp Med* **212**, 1345–1360, doi:10.1084/jem.20151159 (2015).
- Chhabra, A. Mitochondria-centric activation induced cell death of cytolytic T lymphocytes and its implications for cancer immunotherapy. *Vaccine* **28**, 4566–4572, doi:S0264-410X(10)00610-9 (2010).
- Baixaui, F. *et al.* The mitochondrial fission factor dynamin-related protein 1 modulates T-cell receptor signalling at the immune synapse. *EMBO J* **30**, 1238–1250, doi:emboj201125 (2011).
- Kaminski, M. M. *et al.* T cell activation is driven by an ADP-dependent glucokinase linking enhanced glycolysis with mitochondrial reactive oxygen species generation. *Cell Rep* **2**, 1300–1315, doi:10.1016/j.celrep.2012.10.009 (2012).
- Sena, L. A. *et al.* Mitochondria are required for antigen-specific T cell activation through reactive oxygen species signaling. *Immunity* **38**, 225–236, doi:S1074-7613(13)00051-4 (2013).
- Julia, E., Edo, M. C., Horga, A., Montalban, X. & Comabella, M. Differential susceptibility to apoptosis of CD4+ T cells expressing CCR5 and CXCR3 in patients with MS. *Clin Immunol* **133**, 364–374, doi:S1521-6616(09)00773-6 (2009).
- Moodley, D., Mody, G., Patel, N. & Chuturgoon, A. A. Mitochondrial depolarisation and oxidative stress in rheumatoid arthritis patients. *Clin Biochem* **41**, 1396–1401, doi:S0009-9120(08)00300-7 (2008).
- Perl, A., Gergely, P., Jr., Nagy, G., Koncz, A. & Banki, K. Mitochondrial hyperpolarization: a checkpoint of T-cell life, death and autoimmunity. *Trends Immunol* **25**, 360–367, doi:10.1016/j.it.2004.05.001 S1471490604001516 (2004).
- Perl, A., Gergely, P., Jr. & Banki, K. Mitochondrial dysfunction in T cells of patients with systemic lupus erythematosus. *Int Rev Immunol* **23**, 293–313, doi:10.1080/08830180490452576 8H0V7Q1T2M1GQMN0 (2004).
- Nagy, G., Barcza, M., Gonchoroff, N., Phillips, P. E. & Perl, A. Nitric oxide-dependent mitochondrial biogenesis generates Ca²⁺ signaling profile of lupus T cells *J Immunol* **173**, 3676–3683, doi:173/6/3676 (2004).
- Zucchelli, S. *et al.* Defective central tolerance induction in NOD mice: genomics and genetics. *Immunity* **22**, 385–396, doi:S1074-7613(05)00065-8 (2005).
- Pandarpurkar, M. *et al.* I α n4 is required for mitochondrial integrity and T cell survival. *Proc Natl Acad Sci USA* **100**, 10382–10387, doi:10.1073/pnas.18321701001832170100 (2003).
- Nagy, G., Koncz, A. & Perl, A. T cell activation-induced mitochondrial hyperpolarization is mediated by Ca²⁺ - and redox-dependent production of nitric oxide. *J Immunol* **171**, 5188–5197 (2003).
- Gill, T. & Levine, A. D. Mitochondria-derived Hydrogen Peroxide Selectively Enhances T Cell Receptor-initiated Signal Transduction. *J Biol Chem* **288**, 26246–26255, doi:M113.476895 (2013).
- Warburg, O. On the origin of cancer cells. *Science* **123**, 309–314 (1956).
- Chang, C. H. *et al.* Posttranscriptional control of T cell effector function by aerobic glycolysis. *Cell* **153**, 1239–1251, doi:10.1016/j.cell.2013.05.016 (2013).
- MacIver, N. J., Michalek, R. D. & Rathmell, J. C. Metabolic regulation of T lymphocytes. *Annu Rev Immunol* **31**, 259–283, doi:10.1146/annurev-immunol-032712-095956 (2013).
- Nisoli, E. *et al.* Mitochondrial biogenesis in mammals: the role of endogenous nitric oxide. *Science* **299**, 896–899, doi:10.1126/science.1079368 (2003).
- Brown, G. C. Nitric oxide and mitochondrial respiration. *Biochim Biophys Acta* **1411**, 351–369 (1999).
- Quintana, A. *et al.* T cell activation requires mitochondrial translocation to the immunological synapse. *Proc Natl Acad Sci USA* **104**, 14418–14423, doi:0703126104 (2007).
- Schwindling, C., Quintana, A., Krause, E. & Hoth, M. Mitochondria positioning controls local calcium influx in T cells. *J Immunol* **184**, 184–190, doi:jimmunol.0902872 (2010).
- Terasaki, M. & Reese, T. S. Characterization of endoplasmic reticulum by co-localization of BiP and dicarbocyanine dyes. *J Cell Sci* **101**(Pt 2), 315–322 (1992).
- Johnson, L. V., Walsh, M. L., Bockus, B. J. & Chen, L. B. Monitoring of relative mitochondrial membrane potential in living cells by fluorescence microscopy. *J Cell Biol* **88**, 526–535 (1981).
- Gergely, P., Jr. *et al.* Mitochondrial hyperpolarization and ATP depletion in patients with systemic lupus erythematosus. *Arthritis Rheum* **46**, 175–190, doi:10.1002/1529-0131(200201)46:1<175::AID-ART10015>3.0.CO;2-H (2002).
- Nel, A. E. T-cell activation through the antigen receptor. Part 1: signaling components, signaling pathways, and signal integration at the T-cell antigen receptor synapse. *J Allergy Clin Immunol* **109**, 758–770, doi:S0091674902381818 (2002).
- Nel, A. E. & Slaughter, N. T-cell activation through the antigen receptor. Part 2: role of signaling cascades in T-cell differentiation, anergy, immune senescence, and development of immunotherapy. *J Allergy Clin Immunol* **109**, 901–915, doi:S0091674902000015 (2002).
- Haskins, K. & Cooke, A. CD4 T cells and their antigens in the pathogenesis of autoimmune diabetes. *Curr Opin Immunol* **23**, 739–745, doi:S0952-7915(11)00107-5 (2011).
- Zhu, J., Yamane, H. & Paul, W. E. Differentiation of effector CD4 T cell populations (*). *Annu Rev Immunol* **28**, 445–489, doi:10.1146/annurev-immunol-030409-101212 (2010).
- Tse, H. M. *et al.* NADPH oxidase deficiency regulates Th lineage commitment and modulates autoimmunity. *J Immunol* **185**, 5247–5258, doi:10.4049/jimmunol.1001472 (2010).
- Thayer, T. C. *et al.* Superoxide production by macrophages and T cells is critical for the induction of autoreactivity and type 1 diabetes. *Diabetes* **60**, 2144–2151, doi:10.2337/db10-1222 (2011).
- Padgett, L. E., Broniowska, K. A., Hansen, P. A., Corbett, J. A. & Tse, H. M. The role of reactive oxygen species and proinflammatory cytokines in type 1 diabetes pathogenesis. *Ann N Y Acad Sci* **1281**, 16–35, doi:10.1111/j.1749-6632.2012.06826.x (2013).
- Brown, G. C. Regulation of mitochondrial respiration by nitric oxide inhibition of cytochrome c oxidase. *Biochim Biophys Acta* **1504**, 46–57 (2001).
- Brown, G. C. & Borutaite, V. Nitric oxide inhibition of mitochondrial respiration and its role in cell death. *Free Radic Biol Med* **33**, 1440–1450 (2002).
- Ledderose, C. *et al.* Mitochondria are gate-keepers of T cell function by producing the ATP that drives purinergic signaling. *J Biol Chem* **289**, 25936–25945, doi:10.1074/jbc.M114.575308 (2014).
- Wang, R. *et al.* The transcription factor Myc controls metabolic reprogramming upon T lymphocyte activation. *Immunity* **35**, 871–882, doi:10.1016/j.immuni.2011.09.021 (2011).
- Perl, A., Hanczko, R., Telarico, T., Oaks, Z. & Landas, S. Oxidative stress, inflammation and carcinogenesis are controlled through the pentose phosphate pathway by transaldolase. *Trends Mol Med* **17**, 395–403, doi:10.1016/j.molmed.2011.01.014 (2011).
- Vander Heiden, M. G., Cantley, L. C. & Thompson, C. B. Understanding the Warburg effect: the metabolic requirements of cell proliferation. *Science* **324**, 1029–1033, doi:10.1126/science.1160809 (2009).
- Fuss, I. J., Kanof, M. E., Smith, P. D. & Zola, H. Isolation of whole mononuclear cells from peripheral blood and cord blood. *Curr Protoc Immunol* Chapter 7, Unit 7 1, doi:10.1002/0471142735.im0701s85 (2009).

41. de la Tour, D. *et al.* Beta-cell differentiation from a human pancreatic cell line *in vitro* and *in vivo*. *Mol Endocrinol* **15**, 476–483, doi:10.1210/mend.15.3.0604 (2001).
42. Halvorsen, T. L., Leibowitz, G. & Levine, F. Telomerase activity is sufficient to allow transformed cells to escape from crisis. *Mol Cell Biol* **19**, 1864–1870 (1999).

Acknowledgements

We would like to thank Dr. Amanda Posgai (University of Florida) for her assistance in manuscript preparation. This study was supported by Grants # 1-11-BS-104 (CEM), ADA_1-15-TS-22 (CEM) and # 7-12-IN-09 (JC) from the American Diabetes Association, Grants # 17-2012-595 (JC) and 2-2012-280 (TMB) from the Juvenile Diabetes Research Foundation, as well as grants R01 DK074656 (CEM), UC4 DK104194 (CEM), and P01 AI042288 (TMB/MAA/CEM) from the National Institutes of Health. Participation in the project of RJC was supported by a training grant from the National Institutes of Health, T35 HL007489.

Author Contributions

J.C.– researched the data and wrote the manuscript. A.V.C.– researched data and edited the manuscript, J.L.–researched data and edited the manuscript, M.R.K.– researched data and edited the manuscript, R.J.C.– researched data and edited the manuscript, D.J.P.– researched data and edited the manuscript, A.B.M.– Provided clinical samples and edited the manuscript, M.A.A. and T.M.B.– contributed to discussions and edited the manuscript, C.E.M.– developed the initial hypothesis, researched data, contributed to discussions, and contributed to the writing and editing of the manuscript.

Additional Information

Supplementary information accompanies this paper at doi:10.1038/s41598-017-11056-9

Competing Interests: The authors declare that they have no competing interests.

Publisher's note: Springer Nature remains neutral with regard to jurisdictional claims in published maps and institutional affiliations.



Open Access This article is licensed under a Creative Commons Attribution 4.0 International License, which permits use, sharing, adaptation, distribution and reproduction in any medium or format, as long as you give appropriate credit to the original author(s) and the source, provide a link to the Creative Commons license, and indicate if changes were made. The images or other third party material in this article are included in the article's Creative Commons license, unless indicated otherwise in a credit line to the material. If material is not included in the article's Creative Commons license and your intended use is not permitted by statutory regulation or exceeds the permitted use, you will need to obtain permission directly from the copyright holder. To view a copy of this license, visit <http://creativecommons.org/licenses/by/4.0/>.

© The Author(s) 2017